Advance Publication

The Journal of Veterinary Medical Science

Accepted Date: 23 July 2019

J-STAGE Advance Published Date: 23 August 2019

Virology

Note

Feline coronavirus isolates from a part of Brazil: insights into molecular epidemiology and phylogeny inferred from the *7b gene*

INSIGHTS INTO BRAZILIAN FELINE CORONAVIRUS

Luciana MYRRHA[1] · Fernanda SILVA[1] · Pedro VIDIGAL[2] · Maurício RESENDE[3] · Gustavo BRESSAN[1] · Juliana FIETTO[1] · Marcus SANTOS[4] · Laura SILVA[4] · Viviane ASSAO[4] · Abelardo SILVA JUNIOR[4] · Márcia DE ALMEIDA[1]

Address: Federal University of Viçosa (UFV), Peter Henry Rolfs Avenue, Viçosa, Minas Gerais 36570-900, Brazil

[1] Laboratory of Animal Molecular Infectology, Institute of Biotechnology Applied to Agriculture, Federal University of Viçosa (UFV), Viçosa, Minas Gerais 36570-900, Brazil

[2] Nucleus of Analysis of Biomolecules, Center of Biological Sciences, Federal University of Viçosa (UFV), Viçosa, Minas Gerais 36570-900, Brazil

[3] Departament of Microbiology, Federal University of Minas Gerais (UFMG), Belo Horizonte, Minas Gerais 31275-035, Brazil

[4] Laboratory of Immunobiological and Animal Virology, Departament of Veterinary, Federal University of Viçosa (UFV), Viçosa, Minas Gerais 36570-900, Brazil

Corresponding author

Abelardo Silva Júnior

Departament of Veterinary, Federal University of Viçosa (UFV)

Peter Henry Rolfs Avenue, Viçosa, Minas Gerais 36570-900, Brazil

Phone +55 31 38991471

E-mail abelardo.junior@ufv.br

ABSTRACT

The *Feline coronavirus* (FCoV) can lead to Feline infectious peritonitis (FIP), which the precise cause is still unknown. The theory of internal mutation suggests that a less virulent biotype of FCoV (FECV) would lead to another more pathogenic biotype (FIPV) capable of causing FIP. In this work, the *7b gene* was amplified from 51 domestic cat plasma samples by semi-nested PCR and tested through phylogenetic and phylogeographical approaches. The *7b gene* of Brazilian isolates displayed high conservation, a strong correlation between the geographic origin of the viral isolates and their genealogy, and its evolution was possibly shaped by a combination of high rates of nucleotide substitution and purifying selection.

KEYWORDS

7b gene · *Feline coronavirus* · molecular epidemiology · phylogeny

The *Feline coronavirus* (FCoV) is an important pathogen of domestic and wild felids, which can cause subclinical infection, mild enteritis or lead to feline infectious peritonitis (FIP), a fatal disease characterized by inflammatory lesions of serous membranes and systemic granulomatous lesions of parenchymatous organs [23].

Although the precise cause of FIP pathogenesis is still unknown, several hypotheses have been suggested [20]. The most accepted hypothesis, called internal mutation theory, suggests that during the replication of FCoV in the intestinal epithelium, a mutation occurs that makes the virus more pathogenic and able to infect monocytes and macrophages and cause FIP [23, 27]. This virulent mutant variant was designated *Feline infectious peritonitis virus* (FIPV), while a variant that leads to enteric infection has been termed *Feline enteric coronavirus* (FECV) [25]. The precise nature of the mutation responsible for the pathogenesis has not been identified in the FCoV genome [10]. Nevertheless, it has been deduced that the non-structural glycoprotein 7b, codified by ORF7b, plays a determinative role in FCoV virulence [31], besides having a strong phylogenetic sign for the differentiation between FECV and FIPV [3].

To better understand the molecular epidemiology of FCoV in Brazilian domestic cats, phylogenetic hypothesis and viral population dynamics were inferred from the *7b gene*. A phylogenetic hypothesis and the reconstructed population history of FCoV isolates are presented in this work, providing insights into the origins of FCoV in Brazil. Furthermore, the molecular analysis of *7b gene* dispenses considerations about the internal mutation theory, regarding to the virulence of the serotypes of FCoV.

This study included samples from 210 domestic cats (*Felis catus*) of various breeds, random selected from different local animal hospitals (Minas Gerais, Brazil)

during 2003-2010. One hundred twenty-nine animals were healthy and taken to veterinary clinics for vaccinations and/or elective surgery. Eighty-one of them showed clinical symptoms of FIP such as anorexia, weight loss, jaundice, recurrent fever, iritis, or neurological signs and abdominal or pleural effusion [17, 23].

Blood samples were obtained by venipuncture and collected in tubes with ethylenediaminetetraacetic acid (EDTA). The plasma was obtained and frozen at -80 ºC. The collection procedures were performed according to the Ethical Principles in Animal Research of the School of Veterinary Medicine of the University of Viçosa (register number 34/2010). Viral sequences isolated from healthy animals or those with clinical symptoms of FIP were designated as FECV and FIPV sequences, respectively.

The complete accessory protein *7b gene* (766 nt) was amplified by semi-nested PCR with two rounds of amplification using two pairs of primers previously described by Lin and others [17]. The reaction products of the semi-nested PCR were purified and sequenced by Macrogen Inc., Seoul, Korea. Contigs of the nucleotide sequences were assembled using Phred [12] and Phrap (http://www.phrap.org). The complete *7b gene* coding sequences were submitted to GenBank (JX239089- JX239139).

The *7b gene* complete sequences of 58 FCoV isolates were downloaded from GenBank (http://www.ncbi.nlm.nih.gov/Genbank). Thus, the final dataset selected contained 109 *7b gene* sequences, including the sequences of Brazilian isolates.

Phylogenetic evidence for recombination was tested, and recombination breakpoints were predicted using different methods ($P < 0.01$) available in RDP3 version 3.44 [19], including RDP [18], GENECONV [21], MaxChi [28], and Bootscan/Recscan [20]. Only those recombination events predicted by at least three of the methods were taken as valid; the recombinant sequences were removed from the dataset in codon selection analysis.

Selective pressure on each codon of the *7b gene* sequence was evaluated using the difference between non-synonymous (dN) and synonymous (dS) substitution rates per codon using the single-likelihood ancestor counting (SLAC), fixed-effects likelihood (FEL), and internal branches fixed-effects likelihood (IFEL) methods found in DataMonkey (http://www.datamonkey.org/).

Phylogenetic hypotheses for the *7b gene* were inferred by Bayesian inference (BI) and maximum likelihood (ML) (Figure 1) using MrBayes v3.1.2 [16] and GARLI 2.0 [34], respectively. The *7b gene* sequence of canine coronavirus (GenBank ID: GU146061) was added to the dataset as an out-group taxon to root the phylogenetic trees.

Sequences were aligned using MUSCLE v.3.8.31 9 [11]. Sites with gaps were excluded. To expedite the construction of phylogenetic trees, a model of nucleotide substitution was estimated using the jModelTest program [5]. The TIM3ef+I+G substitution model was selected as the best DNA evolution model according to the AIC, AICc, and BIC criteria.

The BI phylogenetic trees were calculated using the Bayesian Markov Chain Monte Carlo (MCMC) method, in two runs with 50,000,000 generations and a sample frequency of 1.000. At the end of each run, the average standard deviation of the split frequencies was 0.015022. The convergence of the parameters was analyzed in TRACER v1.5.0, and the chains reached a stationary distribution after 500,000 generations. Then, a total of 1% of the trees generated was burned to produce the consensus trees.

The TIM3ef+I+G substitution model was selected in the GARLI settings (ratematrix = (0 1 2 0 3 2); statefrequencies = estimate; ratehetmodel = gamma; numratecats = 4; invariantsites = estimate), and the statistical support of the ML

151 phylogenetic trees was calculated by 1,000 bootstrap replicates. The 50% majority rule
152 consensus trees of all bootstrap replicates were summarized using the SumTrees of
153 DendroPy 3.8.0 [30].

154 The population history of the FCoV isolates was reconstructed using a Bayesian
155 skyline plot (BSP), which estimates changes in the effective population size over time
156 [8]. The BSP analysis was carried out in BEAST v1.7.2 [7] according to the BSP
157 tutorial (http://beast-mcmc.googlecode.com/files/BSP.pdf).

158 Only FCoV sequences were selected in BSP analysis. Sequences were aligned
159 using MUSCLE v.3.8.31 9 [11]. Alignments were manually inspected, and the sites
160 with gaps were excluded. The TPM3uf+I+G substitution model was selected as the best
161 DNA evolution model by jModeltest program [8], according to the AIC, AICc, and BIC
162 criteria.

163 To estimate *7b gene* mutation rates, the years of collection of FCoV isolates were
164 retrieved from GenBank. Three molecular clock model assumptions (strict-clock,
165 Bayesian-relaxed exponential molecular clock, and Bayesian-relaxed lognormal
166 molecular clock) were tested. In each test, a MCMC run (1,000,000,000 generations)
167 was performed considering TPM3uf+I+G as the substitution model, the respective
168 molecular clock model assumption, and BSP as a coalescent tree prior. The high
169 number of generations was selected to reach a large effective sample size (ESS > 200).
170 For this purpose, analyses were processed on graphics processing units (GPUs) in a
171 computational cluster at UFV, using BEAGLE v1.0 (http://code.google.com/p/beagle-
172 lib/) with BEAST v1.7.2.

173 For each test, the convergence of the parameters (including the estimated mutation
174 rate) was analyzed in TRACER v1.5.0, and the chains reached a stationary distribution
175 after 10,000,000 generations. The marginal likelihoods obtained in each test were

compared by Bayes factor calculations [29] with 1,000 bootstrap replicates. The test with the highest Bayes factor corresponds to the best-fit clock model and a better estimation of the mutation rate. Following this, 1% of the trees generated were burned to produce a consensus time-tree (Figure 2) using TreeAnnotator v1.7.2 [7].

To test the influence of geographic structure and of the virulence of strains in the FCoV population, the phylogenetic trees were analyzed in BaTS v1.0 (Bayesian Tip-Significance testing) [22]. In these tests (geographic distribution and virulence), the high credibility set of trees estimated in the BSP MCMC run were selected, and the association index (AI) [33], parsimony score (PS) [27], and maximum monophyletic clade size (MC) [22] were calculated using 10,000 replicates (Table 1).

A total of 210 plasma samples from domestic cats (*F. catus*) were analyzed by semi-nested PCR from the accessory protein *7b gene*. Fifty-one samples were positive for the *7b gene* of FCoV. In the analysis of the positive samples was found a prevalence of asymptomatic cats of 68.63%, and 31.37% of the cats had symptoms of FIP .

In sequence alignments, the *7b genes* of FCoV isolates presented overall identity ranging from 41.33% (excluding sites with gaps) to 50.48% (excluding sequences with gaps).

Estimation of codon selection pressures in the 7b protein showed that 27.67% of codons were predicted to be negative selection sites, with a global dN/dS estimate of 0.306. Purifying selection is indicated by estimation of codon selection pressures in the 7b protein.

The Brazilian isolates presented higher conservation of *7b gene* sequence, with an overall identity of 98.87% in the sequence alignment. Only seven polymorphic sites differentiate the sequences of JX239089 (FECV), JX239090 (FECV), JX239091 (FIPV), and JX239092 (FIPV) from those of the other 47 isolates (33 FECV and 14

FIPV). These polymorphisms result in the following amino acid substitutions in the 7b protein: H160P for JX239089; H48Y for JX239090; S89F, T159N, H160P, Y167D, and C168W for JX239091; and A19S for JX239092.

To describe the correlation between geographic location, virulence of strains, and genealogy estimated by Bayesian analyses, summary statistics were calculated by BaTS [22] (Tables 1 and 2) that correlate the viral phenotypic characters with the shared ancestry (represented by the phylogenetic tree). This correlation was measured by computation of the association index (AI) [33], parsimony score (PS) [27], and maximum monophyletic clade size (MC) [22]. The AI and PS test the association between traits (geographic distribution and virulence) and tree topology. The MC index tests whether traits are associated with phylogeny. Stronger phylogeny–trait associations should produce larger monophyletic clades (MC) sharing the same trait [22].

The *7b gene* phylogenetic trees (Figures 1 and 2) suggest a geographic pattern of the distribution of FCoV viral isolates. All Brazilian isolates (sampled between 2003 and 2010) were included in the same monophyletic clade with two other North American FIPV isolates (NC_002306 and X90573, sampled in 1979 and 1981, respectively) (Fig. 1).

This work provides a comprehensive analysis of the molecular epidemiology of FCoV isolates circulating in Brazil through prediction of the main events of viral introduction, and it provides new insights about viral population dynamics and selection pressures that shaped the evolution of the FCoV *7b gene*.

In sequence alignments, previous studies have suggested a strong correlation between insertions/deletions (indels) in the *7b gene* and the virulence of FCoV viral strains [15, 31, 32]. However, no correlation between indels in the *7b gene* and

226 virulence was found in sequence alignments, as also described by Battilani and others
227 [2], Lin and others [17] and Bank-Wolf and others [1].

228 With higher conservation of *7b gene* sequence, the Brazilian isolates presented
229 only seven polymorphic sites. Most of these polymorphisms were predicted to be
230 neutral sites in the estimation of selection pressure, seeming to be random and not
231 correlated with the virulence of strains. This high conservation of the *7b gene* among
232 Brazilian FCoV isolates shows that the internal mutation theory [1, 23, 31] possibly
233 could not be considered for this gene. According to this theory, virulent strains (FIPV)
234 evolve from avirulent strains (FECV) by mutation during infection in cats.

235 Homologous recombination has an important role in FCoV evolution, and there is
236 evidence of recombinant strains of FCoV that arose from recombination between FCoV
237 and canine coronavirus (CCoV) [14]. In the recombination analysis of 7b sequences by
238 RDP3, only one recombination event, involving three Taiwanese FCoV isolates
239 sampled in 2004, was detected. Isolate DQ675437 (FECV) was predicted to be a
240 recombinant of DQ675439 (FECV) and DQ675429 (FIPV) ($P = 1.636\times10^{-3}$). This
241 finding possibly suggests a low frequency of homologous recombination of the *7b gene*
242 among FCoV strains.

243 Substitution rates also provide good insight into virus evolution, reflecting the
244 restrictions in genetic diversity that lead to variations in adaptability and pathogenicity
245 of the viral population [6]. Bayes factors analysis suggested that the Bayesian-relaxed
246 exponential molecular clock was the best-fit model for the *7b gene* sequences, and the
247 estimated mean substitution rate was $5.686x10^{-4}$ substitutions/site/year. This estimate
248 agrees with what has been described for other RNA viruses, whose rates generally range
249 from 10^{-2} to 10^{-5} substitutions/site/year [9, 13, 26].

250 Although most FECV and FIPV strains were included in monophyletic clades

with other viral isolates that share the same geographic origin (i.e., Brazil, the United Kingdom, the United States, or Taiwan), it was not possible to define monophyletic clades that distinguish FECV and FIPV.

In geographic pattern analysis (Table 1), the topology of the *7b gene* phylogenetic tree was supported by significant values of AI and PS, and all countries, with the exception of the United Kingdom (probably due to the lower sample size), showed differentiated subpopulations supported by significant MC values. In virulence pattern analysis (Table 2), no significant correlations were found by calculation of AI, PS, or MC. Thus, 7b sequences of FCoV isolates are possibly phylogenetically structured according to their geographic origin irrespective of their pathotype as shown by others [1, 2, 4, 17]. These findings contradict the hypothesis of distinct virulent (FIPV) and avirulent (FECV) strains circulating in natural populations of FCoV, proposed by Brown and others [3]. According to this hypothesis, these two viral strains would be expected to be separated into monophyletic clusters in the phylogenetic tree inferred from the *7b gene*.

RNA viruses may present great genetic diversity variation at the population level, allowing the reconstruction of phylogeny that reflects their epidemiological history [6]. In this way, the time tree of Bayesian Skyline analysis predicted the possible events of viral introduction over time (Fig. 2). Different events of viral introduction in Taiwan, the United Kingdom, and the USA occurred between 1850 and 1950 and are highlighted in the phylogenetic time-tree (Fig. 2). These observations are consistent with the epidemiological history of FCoV. After World War II, there was a dramatic shift in the status of cats as pets. The number of pet cats greatly increased, and this is known to favor FCoV infection [24].

A possible source of FCoV introduction in Brazil is based on the inclusion of all

Brazilian isolates in the same monophyletic clade with two North American FIPV isolates (NC_002306 and X90573), witch presented identical sequences to the 47 Brazilian isolates (33 FECV and 14 FIPV) (Fig. 1). According to the phylogenetic time-tree (Fig. 2), the introduction of FCoV in Brazil possibly occurred since 1975.

The authors have shown that Brazilian FCoV isolates were recently introduced from the North America, and that evolution of the *7b gene* was possibly shaped by a combination of high rates of nucleotide substitution ($5.686x10^{-4}$) and purifying selection. Furthermore, the time tree of the present study suggests that FCoV introduction in Brazil occurred over the past of 40 years. Additionally, the findings of the present study suggest that both the internal mutation theory [23, 31] and the hypothesis of distinct virulent (FIPV) and avirulent (FECV) strains circulating [3] possibly cannot be taken as valid for the *7b gene*. The authors have reported high conservation among sequences of Brazilian isolates and a strong correlation between the geographic origin of viral isolates and the genealogy predicted from the *7b gene*. Thus, it is more plausible that FIP is clinically manifested in cats, mainly due to host and environmental factors and independent of genetic differences between FECV and FIPV. Comparative sequence analysis may eventually not be sufficient to answer the FECV/FIPV question.

ACKNOWLEDGMENTS

The authors would like to thank Mauricio Resende from the Laboratory of Comparative Virology (Institute of Biological Sciences, Federal University of Minas Gerais); José Cleydson Ferreira da Silva from BIOAGRO (Federal University of

Vicosa); and the Department of Information Technology (Federal University of Vicosa; http://www.cpd.ufv.br). This research was supported by the Brazilian Government Agencies Coordenação de Aperfeiçoamento de Pessoal de Nível Superior (CAPES), Conselho Nacional de Desenvolvimento Científico e Tecnológico (CNPq) and Fundação de Amparo à Pesquisa do Estado de Minas Gerais (FAPEMIG).

AUTHOR CONTRIBUTIONS

All authors contributed to this work and agreed to its publication.

COMPLIANCE WITH ETHICAL STANDARDS

Conflict of interest: The authors declare that they have no conflict of interest.

REFERENCES

1. Bank-Wolf, B. R., Stallkamp, I., Wiese, S., Moritz, A., Tekes, G., Thiel, H.-J., 2014. Mutations of 3c and spike protein genes correlate with the occurrence of feline infectious peritonitis. *Vet. Microbiol.* **173**: 177–188.
2. Battilani, M., Coradin, T., Scagliarini, A., Ciulli. S., Ostanello, F., Prosperi, S. and Morganti, L. 2003. Quasispecies composition and phylogenetic analysis of feline coronaviruses (FCoVs) in naturally infected cats. *FEMS Immunol. Med. Microbiol.* **39**: 141–147.
3. Brown, M.A., Troyer, J.L., Pecon-Slattery, J., Roelke, M.E. and O'Brien, S.J. 2009.

326 Genetics and pathogenesis of feline infectious peritonitis virus. *Emerg. Infect. Dis.*
327 **15**: 1445–1452.
328 4. Chang, H. W., Egberink, H. F. and Rottier, P. J. M. 2011. Sequence analysis of feline
329 coronaviruses and the circulating virulent/avirulent theory. *Emerg. Infect. Dis.*
330 5. Darriba, D., Taboada, G. L., Doallo, R. and Posada, D. 2012 jModelTest 2: more
331 models, new heuristics and parallel computing. *Nat. Methods* **9**: 772.
332 6. Denison, M. R., Graham, R. L., Donaldson, E. F., Eckerle, L. D. and Baric, R.S.
333 2011. Coronaviruses: an RNA proofreading machine regulates replication fidelity
334 and diversity. *RNA Biol.* **8**: 270–279.
335 7. Drummond, A. J., Suchard, M. A., Xie, D. and Rambaut, A. 2012. Bayesian
336 phylogenetics with BEAUti and the BEAST 1.7. *Mol Biol. Evol.* **29**: 1969–1973.
337 8. Drummond, A. J., Rambaut, A., Shapiro, B. and Pybus, O. G. 2005. Bayesian
338 coalescent inference of past population dynamics from molecular sequences. *Mol.*
339 *Biol. Evol.* **22**: 1185–1192.
340 9. Duffy, S., Shackelton, L. A. and Holmes, E. C. 2008. Rates of evolutionary change
341 in viruses: patterns and determinants. *Nat. Rev. Genet.* **9**: 267–276.
342 10. Dye, C. and Siddell, S. G. 2007. Genomic RNA sequence of *Feline coronavirus*
343 strain FCoV C1Je. *J. Feline Med. Surg.* **9**: 202–213.
344 11. Edgar, R. C. 2004. MUSCLE: multiple sequence alignment with high accuracy and
345 high throughput. *Nucleic Acids Res.* **32**: 1792–1797.
346 12. Ewing, B. and Green, P. 1998. Base-calling of automated sequencer traces using
347 phred. II. Error probabilities. *Genome Res.* **8**: 186–194.
348 13. Hanada, K., Suzuki, Y. and Gojobori, T. 2004. A large variation in the rates of
349 synonymous substitution for RNA viruses and its relationship to a diversity of viral
350 infection and transmission modes. *Mol. Biol. Evol.* **21**: 1074–1080.

14. Herrewegh, A. A., Smeenk, I., Horzinek, M. C., Rottier, P.J. and de Groot, R.J. 1998. *Feline coronavirus* type II strains 79-1683 and 79-1146 originate from a double recombination between *Feline coronavirus* type I and *Canine coronavirus*. *J. Virol.* **72**: 4508–4514.

15. Herrewegh, A. A., Vennema, H., Horzinek, M. C., Rottier, P.J. and de Groot, R. J. 1995. The molecular genetics of feline coronaviruses: comparative sequence analysis of the ORF7a/7b transcription unit of different biotypes. *Virology* **212**: 622–631.

16. Huelsenbeck, J. P. and Ronquist, F. 2001. MRBAYES: Bayesian inference of phylogenetic trees. *Bioinformatics* **17**: 754–755.

17. Lin, C.-N., Su, B.-L., Huang, H.-P., Lee, J.-J, Hsieh, M.-W and Chueh, L.-L. 2009. Field strain feline coronaviruses with small deletions in ORF7b associated with both enteric infection and feline infectious peritonitis. *J. Feline Med. Surg.* **11**: 413–419.

18. Martin, D. and Rybicki, E. 2000. RDP: detection of recombination amongst aligned sequences. *Bioinformatics* **16**: 562–563.

19. Martin, D. P., Lemey, P., Lott, M., Moulton, V., Posada, D. and Lefeuvre, P. 2010. RDP3: a flexible and fast computer program for analyzing recombination. *Bioinformatics* **26**: 2462–2463.

20. Myrrha, L. W., Silva, F. M. F., Peternelli, E. F. D. O., Junior, A. S., Resende, M., and de Almeida, M. R., 2011. The paradox of feline coronavirus pathogenesis: a review. *Adv. Virol.* 2011, 109849.

21. Padidam, M., Sawyer, S. and Fauquet, C. M. 1999. Possible emergence of new geminiviruses by frequent recombination. *Virology* **265**: 218–225.

22. Parker, J., Rambaut, A. and Pybus, O. G. 2008. Correlating viral phenotypes with phylogeny: accounting for phylogenetic uncertainty. Infect. Genet. Evol. **8**: 239–246.

23. Pedersen, N. C. 2009. A review of feline infectious peritonitis virus infection:

1963–2008. *J. Feline Med. Surg.* **11**: 225–258.

24. Pedersen, N. C., Allen, C. E. and Lyons, L. A. 2008. Pathogenesis of feline enteric coronavirus infection. *J. Feline Med. Surg.* **10**: 529–541.

25. Poland, A. M., Vennema, H., Foley, J. E. and Pedersen, N. C., 1996. Two related strains of feline infectious peritonitis virus isolated from immunocompromised cats infected with a feline enteric coronavirus. *J. Clin. Microbiol.* **34**: 3180–3184.

26. Silva, F. M., Vidigal, P.M., Myrrha, L. W., Fietto, J. L., Silva Junior, A. and Almeida, M. R. 2013. Tracking the molecular epidemiology of Brazilian Infectious bursal disease virus (IBDV) isolates. *Infect. Genet. Evol.* **13**: 18–26.

27. Slatkin, M. and Maddison, W. P. 1989. A cladistic measure of gene flow inferred from the phylogenies of alleles. *Genetics* **123**: 603–613.

28. Smith, J. M. 1992. Analyzing the mosaic structure of genes. *J. Mol. Evol.* **34**: 126–129.

29. Suchard, M. A., Weiss, R. E. and Sinsheimer, J. S. 2001. Bayesian selection of continuous-time Markov chain evolutionary models. *Mol. Biol. Evol.* **18**: 1001–1013.

30. Sukumaran, J. and Holder, M. T. 2010. DendroPy: a Python library for phylogenetic computing. *Bioinformatics* **26**: 1569–1571.

31. Vennema, H., Poland, A., Foley, J. and Pedersen, N. C., 1998. Feline infectious peritonitis viruses arise by mutation from endemic feline enteric coronaviruses. *Virology* **243**: 150–157.

32. Vennema, H., Rossen, J. W., Wesseling, J., Horzinek, M. C. and Rottier, P. J. 1992. Genomic organization and expression of the 3’ end of the canine and feline enteric coronaviruses. *Virology* **191**: 134–140.

33. Wang, T. H., Donaldson, Y. K., Brettle, R. P., Bell, J. E. and Simmonds, P. 2001. Identification of shared populations of human immunodeficiency virus type 1

infecting microglia and tissue macrophages outside the central nervous system. *J. Virol.* **75**: 11686–11699.

34. Zwickl, D. J. 2006. Genetic algorithm approaches for the phylogenetic analysis of large biological sequence datasets under the maximum likelihood criterion. Dissertation, The University of Texas at Austin.

FIGURES LEGENDS

Fig.1 Evolutionary relationships between *Feline coronavirus* (FCoV) isolates based on the *7b gene*. The majority-rule consensus tree was obtained by Bayesian MCMC coalescent analysis of 109 complete *7b gene* sequences. The posterior probability values (PP) (bold; expressed as percentages) calculated using the best trees found by MrBayes are shown beside each node. The second value corresponds to the bootstrap value (BV) (underlined; expressed as percentage) that defines the clusters in the maximum likelihood tree. The outgroup taxon is an isolate of canine coronavirus (GenBank ID: GU146061).

Fig.2 Time tree of *Feline coronavirus* (FCoV) isolates reconstructed from the *7b gene*. The majority-rule consensus tree of the *7b gene* was obtained by a coalescent Bayesian skyline analysis with an exponential molecular clock model assumption using BEAST. The colors of branches indicate the geographic origin of the FCoV isolates

422 **Fig1.**

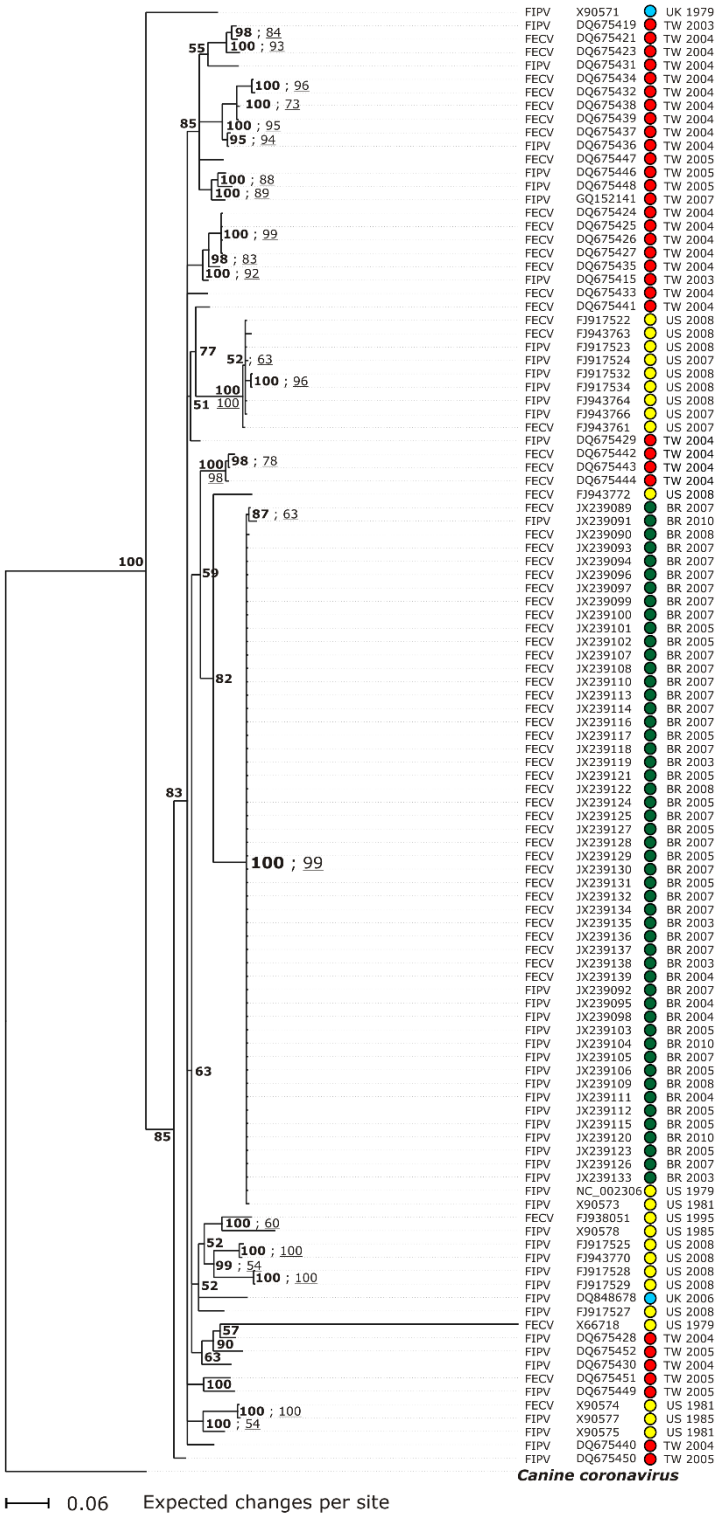
FIPV X90571 UK 1979
FIPV DQ675419 TW 2003
FECV DQ675421 TW 2004
FECV DQ675423 TW 2004
FIPV DQ675431 TW 2004
FECV DQ675434 TW 2004
FECV DQ675432 TW 2004
FECV DQ675438 TW 2004
FECV DQ675439 TW 2004
FECV DQ675437 TW 2004
FIPV DQ675436 TW 2004
FECV DQ675447 TW 2005
FIPV DQ675446 TW 2005
FIPV DQ675448 TW 2005
FIPV GQ152141 TW 2007
FECV DQ675424 TW 2004
FECV DQ675425 TW 2004
FECV DQ675426 TW 2004
FECV DQ675427 TW 2004
FECV DQ675435 TW 2004
FIPV DQ675415 TW 2003
FECV DQ675433 TW 2004
FECV DQ675441 TW 2004
FECV FJ917522 US 2008
FECV FJ943763 US 2008
FIPV FJ917523 US 2008
FIPV FJ917524 US 2007
FIPV FJ917532 US 2008
FIPV FJ917534 US 2008
FIPV FJ943764 US 2008
FIPV FJ943766 US 2007
FECV FJ943761 US 2007
FIPV DQ675429 TW 2004
FECV DQ675442 TW 2004
FECV DQ675443 TW 2004
FECV DQ675444 TW 2004
FECV FJ943772 US 2008
FECV JX239089 BR 2007
FIPV JX239091 BR 2010
FECV JX239090 BR 2008
FECV JX239093 BR 2007
FECV JX239094 BR 2007
FECV JX239096 BR 2007
FECV JX239097 BR 2007
FECV JX239099 BR 2007
FECV JX239100 BR 2007
FECV JX239101 BR 2005
FECV JX239102 BR 2005
FECV JX239107 BR 2007
FECV JX239108 BR 2007
FECV JX239110 BR 2007
FECV JX239113 BR 2007
FECV JX239114 BR 2007
FECV JX239116 BR 2007
FECV JX239117 BR 2005
FECV JX239118 BR 2007
FECV JX239119 BR 2003
FECV JX239121 BR 2005
FECV JX239122 BR 2008
FECV JX239124 BR 2005
FECV JX239125 BR 2007
FECV JX239127 BR 2005
FECV JX239128 BR 2007
FECV JX239129 BR 2005
FECV JX239130 BR 2007
FECV JX239131 BR 2005
FECV JX239132 BR 2007
FECV JX239134 BR 2007
FECV JX239135 BR 2003
FECV JX239136 BR 2007
FECV JX239137 BR 2007
FECV JX239138 BR 2003
FECV JX239139 BR 2004
FIPV JX239092 BR 2007
FIPV JX239095 BR 2004
FIPV JX239098 BR 2004
FIPV JX239103 BR 2005
FIPV JX239104 BR 2010
FIPV JX239105 BR 2007
FIPV JX239106 BR 2005
FIPV JX239109 BR 2008
FIPV JX239111 BR 2004
FIPV JX239112 BR 2005
FIPV JX239115 BR 2005
FIPV JX239120 BR 2010
FIPV JX239123 BR 2005
FIPV JX239126 BR 2007
FIPV JX239133 BR 2003
FIPV NC_002306 US 1979
FIPV X90573 US 1981
FECV FJ938051 US 1995
FIPV X90578 US 1985
FIPV FJ917525 US 2008
FIPV FJ943770 US 2008
FIPV FJ917528 US 2008
FIPV FJ917529 US 2008
FIPV DQ848678 UK 2006
FIPV FJ917527 US 2008
FECV X66718 US 1979
FIPV DQ675428 TW 2004
FIPV DQ675452 TW 2005
FIPV DQ675430 TW 2004
FECV DQ675451 TW 2005
FIPV DQ675449 TW 2005
FECV X90574 US 1981
FIPV X90577 US 1985
FIPV X90575 US 1981
FIPV DQ675440 TW 2004
FIPV DQ675450 TW 2005
Canine coronavirus
0.06 Expected changes per site

423

424 **Fig2.**

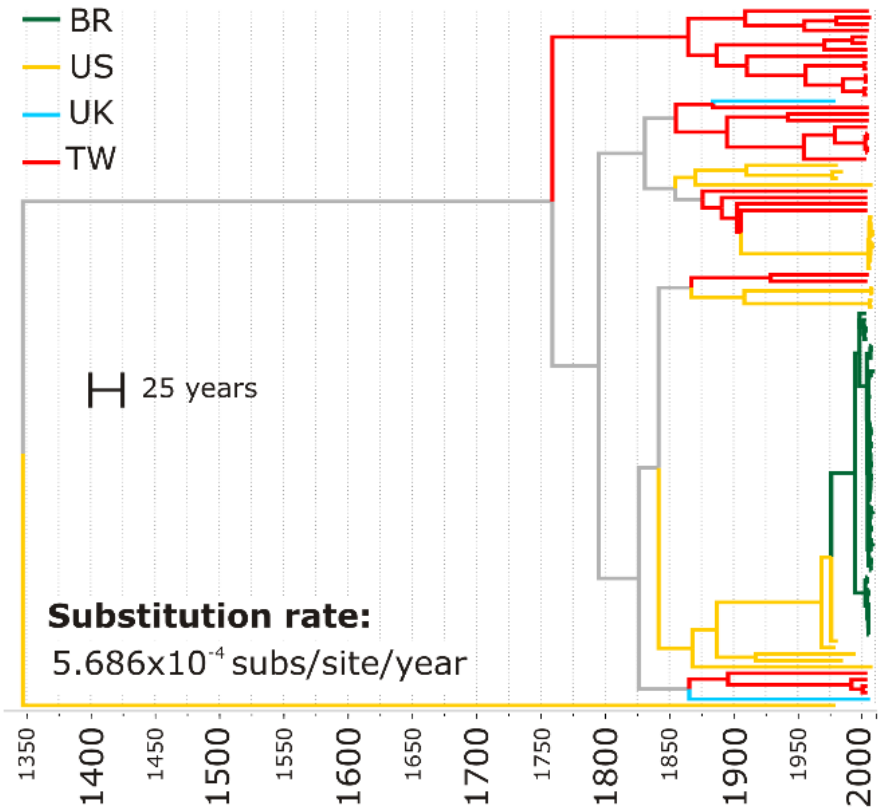
BR
US
UK
TW
25 years
Substitution rate:
5.686x10-4 subs/site/year
1350
1400
1450
1500
1550
1600
1650
1700
1750
1800
1850
1900
1950
2000

425

426

Table1. Geographic effect on the population structure of *Feline coronavirus* (FCoV) isolates.

Tested correlation	Statistics [a]	Observed	Expected [b]	P-value*
Geographic origin	AI	0.2413 (0.0125; 0.5361)	7.4867 (6.6256; 8.2920)	0
Geographic origin	PS	7.65 (6.0000; 9.0000)	48.5762 (45.6100; 51.2300)	0
Taiwan	MC	15.11 (14.0000; 23.0000)	2.4121 (2.0200; 3.2400)	1.00E-04
United States	MC	9.25 (9.0000; 12.0000)	1.9445 (1.4700; 2.3500)	1.00E-04
United Kingdom	MC	1 (1.0000; 1.0000)	1.005 (1.0000; 1.0200)	1
Brazil	MC	46.85 (29.0000; 51.0000)	3.5105 (2.7300; 4.5900)	1.00E-04

The numbers in parentheses correspond to the 95% lower and upper bounds of the highest-probability density intervals.

[a]AI: association index; PS: parsimony score; MC: maximum monophyletic clade;

[b]Expected value on null hypothesis (random phylogeny-trait association).

[*]Statistical significance of tests: P <0.01.

427

Table 2. Effect of virulence on the population structure of *Feline coronavirus* (FCoV) isolates.

Tested correlation	Statistics [a]	Observed	Expected [b]	P-value*
Virulence	AI	4.8142 (3.7616; 5.7645)	5.6474 (4.7441; 6.5434)	0.07
Virulence	PS	32.03 (29,0000; 34.0000)	36.0344 (32,8600; 38.87004)	0.02
FECV[I]	MC	5.81 (5.0000; 9.0000)	4.2245 (3.3500; 6.0200)	0.1
FIPV[II]	MC	4.46 (4.0000; 6.0000)	3.3531 (2.6200; 4.3200)	0.15

The numbers in parentheses correspond to the 95% lower and upper bounds of the highest-probability density intervals.

[a] AI: association index; PS: parsimony score; MC: maximum monophyletic clade;

[b] Expected value on null hypothesis (random phylogeny-trait association).

[I] Less-pathogenic biotype of FCoV

[II] Pathogenic biotype of FCoV

[*] Statistical significance of tests: P <0.01.

428